

Abstract

The initiation of fractures and fast flow in floating regions of Antarctica have the potential to destabilize large regions of the grounded ice sheet, leading to significant sea-level rise. While observations have shown rapid, localized deformation and damage in the margins of fast-flowing glaciers, there remain gaps in our understanding of how rapid deformation affects the viscosity and toughness of ice. Here we derive a model for dynamic recrystallization of ice that includes a novel representation of migration recrystallization. This mechanism is absent from existing models and is likely dominant in warm areas undergoing rapid deformation, such as shear margins in ice sheets. While solid earth studies find fine-grained rock in shear zones, here we find elevated ice grain sizes (> 10 mm) due to warmer temperatures and high strain rates activating migration recrystallization. Large grain sizes implies that ice in shear margins deforms primarily by dislocation creep, suggesting a flow-law stress exponent of $n \approx 4$ rather than the canonical $n = 3$. Further, we find that this increase in grain size results in a decrease in tensile strength of ice by $\sim 75\%$ in the margins of glaciers. Thus, this increase in grain size softens the margins of fast-flowing glaciers and makes ice shelf margins more vulnerable to fracture than previously supposed. These results also suggest the need to consider the effects of dynamic recrystallization in large-scale ice-sheet modeling.

Introduction

Ice shelves, the floating regions of large ice sheets, provide a significant control on the evolution of ice sheets and their contributions to sea-level rise. Ice shelves restrain (i.e., buttress) the upstream grounded portions of the ice sheet, preventing rapid flow of grounded ice towards the ocean. Calving events and dynamic thinning reduce the buttressing that ice shelves provide to the grounded ice, resulting in accelerated flow and possible instability of the ice sheet (Weertman, 1974; Thomas & Bentley, 1978; Scambos, 2004; Rignot, 2004; Schoof, 2007; Pollard et al., 2015). Thus, a combination of ice fracture and accelerated flow may play a significant role in controlling the stability of the West Antarctic Ice Sheet (Thomas & Bentley, 1978; Wingham et al., 2009; Pollard et al., 2015; Gudmundsson et al., 2019; Clerc et al., 2019).

Fracture and flow generally occur in areas of rapid deformation, which appears in the margins of fast-flowing glaciers and ice shelves (known as *shear margins*). A significant concentration of fractures and damage on ice shelves are found in the margins, which may have implications for the stability of the ice shelf (Lhermitte et al., 2020). Further, the lateral shearing that occurs in shear margins of grounded glaciers provides a control on flow speed and contributes to the buttressing effect (MacAyeal, 1989; Ranganathan et al., 2020). While this has been well-observed, there remains uncertainty in the physical processes underlying fracturing and accelerated flow in shear margins.

Fundamentally, the creep and fracture of ice are dictated by the grain-scale microstructure of the ice. It is well-known from solid earth studies that the physical properties of the crystalline microstructure - including grain size and grain orientation - affect the rates of creep and fracture of rocks significantly (Van der Wal et al., 1993; J. H. P. De Bresser et al., 1998; J. De Bresser et al., 2001; Montési & Hirth, 2003; Warren et al., 2008; Skemer et al., 2013) and modeling and laboratory studies have proposed similar effects in ice (Currier & Schulson, 1982; W. Nixon & Schulson, 1987; Wu & Niu, 1995; K. M. Cuffey et al., 2000; Montagnat & Duval, 2000; D. L. Goldsby & Kohlstedt, 2001; Duval et al., 2010; Hruby et al., 2020; Behn et al., 2020). However, the physics of the microstructure of ice has rarely been applied to the question of how rapid deformation induces positive feedbacks on flow and how areas of rapid deformation fracture. Here, we study the effect that deformation-induced grain size evolution may have on flow and fracture of ice.

57 Observations show that grains are large in areas of glaciers where ice is warm and
 58 being sheared. Measurements of grain size in the GRIP (Greenland Ice Core Project)
 59 ice core and GISP2 (Greenland Ice Sheet Project 2) ice core shows that grain sizes in-
 60 crease rapidly with depth near the base, where the ice is frozen to the bed and thus strain
 61 rates are relatively large and the ice is warm (Thorsteinsson et al., 1997; Gow et al., 1997).
 62 We would therefore expect grains to be large in shear margins, where strain rates are
 63 quite high (Gardner et al., 2018) and consequently the ice is warmed, sometimes to the
 64 melting point, through viscous dissipation (Meyer & Minchew, 2018). While there are
 65 no observations of grain size at depth in shear margins, measurements made in shallow
 66 boreholes (Jackson & Kamb, 1997) and observations of grain size in temperate glaciers
 67 (Tison & Hubbard, 2000) support the suggestion that grains are likely large in shear mar-
 68 gins.

69 Grain size influences the mechanisms of creep that allow ice to flow as a viscous
 70 fluid (D. L. Goldsby & Kohlstedt, 2001). Most known creep mechanisms, such as dif-
 71 fusion creep and grain-boundary sliding, have explicit and well-tested grain size depen-
 72 dencies. On the other hand, numerous laboratory experiments have shown that dislo-
 73 cation creep is practically independent of grain size (Duval & Gac, 1980; T. Jacka, 1984).
 74 For grain-size-dependent mechanisms, creep deformation is enhanced as grain sizes get
 75 smaller and diminished as grain sizes grow. Therefore, there is a tendency to dislocation
 76 creep as grain size grows and we may expect that areas of large grain sizes will deform
 77 primarily by dislocation creep, a consideration with important implications for the vis-
 78 cosity of ice. Since rates of shearing in shear margins affect the flow speed of grounded
 79 ice and may affect the buttressing of ice shelves, grain size in shear margins may also af-
 80 fect ice shelf evolution.

81 Furthermore, the tendency for ice to fracture is a function of the size and distri-
 82 bution of flaws, where stresses intensify. Larger flaw sizes tend to increase the stress in-
 83 tensity, implying that in general, the tensile strength of ice decreases as the flaw size in-
 84 creases. For intact or pristine ice, the flaw size is set by the grain size, and therefore the
 85 tensile strength of ice decreases as grain size increases, consistent with laboratory stud-
 86 ies (Figure 3a) (Currier & Schulson, 1982; W. Nixon & Schulson, 1987; W. A. Nixon &
 87 Schulson, 1988). Thus, we might suppose that glacier shear margins are likely to have
 88 relatively large grain sizes that will decrease the tensile strength of the ice and could ex-
 89 plain the observations of crevassing and fracture (e.g. (Lhermitte et al., 2020)). Here,
 90 we derive a model for steady-state grain size in deforming glacier ice to consider the ef-
 91 fect that grain size may have on the creep and vulnerability of ice to fracture in shear
 92 margins of rapidly-deforming glaciers.

93 **A Steady-State Grain Size Model**

94 Recrystallization processes alter the orientation and size of ice grains both in the absence
 95 of and in response to deformation. While there are many mechanisms of recrystalliza-
 96 tion, three main mechanisms likely dominate the evolution of grain size in ice: normal
 97 grain growth, rotation recrystallization, and migration recrystallization (Duval & Castel-
 98 nau, 1995). Thus the net rate of change in grain size can be described as the sum of the
 99 contributions from all mechanisms, assuming that these mechanisms operate indepen-
 100 dently, as past work has assumed (Austin & Evans, 2007):

$$\dot{d} = \dot{d}_{rot} + \dot{d}_{mig} + \dot{d}_{nor} \quad (1)$$

101 where overdots represent time derivatives, \dot{d}_{nor} is the rate of change in grain size due to
 102 normal grain growth, \dot{d}_{rot} is the rate of change in grain size due to rotation recrystal-
 103 lization, and \dot{d}_{mig} is the rate of change in grain size due to migration recrystallization.

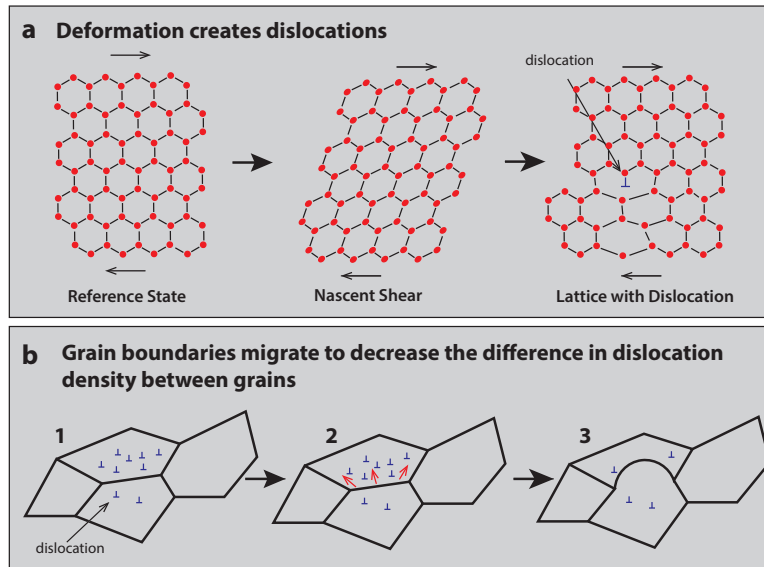


Figure 1. Schematic of migration recrystallization. (a) In response to stress (in Antarctic glaciers, this stress arises from the ice sheet deforming under its own weight), the ice shears, creating dislocations. (b) A hypothetical polycrystalline ice of four grains. Due to local heterogeneities in stress, the density of the resulting dislocations are also heterogeneous [1]. To relieve stresses created by the difference in dislocation density between two grains, the grain boundary migrates towards the area of higher dislocation density [2], absorbing the dislocations and leaving behind a region of zero dislocation density [3]. The fact that the boundary leaves behind a region of no dislocation density may create more heterogeneities in dislocation density, driving further grain boundary migration.

104 In the absence of deformation (static recrystallization), normal grain growth dom-
 105 inates, meaning that grain boundaries migrate outwards, leading to an increase in grain
 106 size (R. Alley, 1992). This migration is driven partially by grain boundary energy γ , which
 107 represents the change in free energy per change in unit area of the grain (Jellinek & Gouda,
 108 1969; Ohtomo & Wakahama, 1983; Duval, 1985; R. Alley et al., 1986b, 1986a). In con-
 109 trast, deformation activates the two other recrystallization mechanisms (dynamic recryst-
 110 tallization) through the introduction of dislocations into the ice crystalline lattice. In an
 111 incompressible material such as ice, the rate of work done during deformation is defined
 112 as the double inner product $\tau_{ij}\dot{\epsilon}_{ij}$ (in summation notation), where τ_{ij} is the deviatoric
 113 stress tensor and $\dot{\epsilon}_{ij}$ is the strain rate tensor. The work rate is a combination of the change
 114 in internal energy from migration recrystallization and rotation recrystallization, described
 115 mathematically as

$$(1 - \Theta)\tau_{ij}\dot{\epsilon}_{ij} = \dot{E}_{rot} - \dot{E}_{mig} \quad (2)$$

116 where Θ represents the fraction of the work rate that is dissipated as heat, \dot{E}_{rot} is the
 117 rate of change in internal energy due to rotation recrystallization, and \dot{E}_{mig} is the rate
 118 of change in internal energy due to migration recrystallization. Rotation recrystalliza-
 119 tion reduces grain size: dislocations align to form subgrain boundaries, and as the lat-
 120 tice rotates, these subgrain boundaries can form a new grain boundary (Duval & Castel-
 121 nau, 1995). Migration recrystallization, on the other hand, grows grains: grain-scale stress
 122 gradients cause heterogeneity in dislocation density within the grain, which result in stress
 123 gradients that drive the outward migration of boundaries. This mechanism is dominant
 124 at high temperatures and high strain, where dislocation density is likely to be most het-
 125 erogeneous (Duval, 1985; R. Alley, 1988). Since rotation and migration recrystallization
 126 have opposite effects on surface energy, the two energy rates have opposite signs (dis-
 127 cussed more in detail in Supplement Section A).

128 Here, we build upon the steady-state grain size model from (Austin & Evans, 2007)
 129 by adding a parameterization for migration recrystallization, allowing us to predict grain
 130 size in shear margins. Migration recrystallization occurs when the temperature of the
 131 material approaches the melting temperature (Duval & Castelnau, 1995; Montagnat &
 132 Duval, 2000). Current steady-state grain size models, such as those derived by (Derby
 133 & Ashby, 1987), (J. H. P. De Bresser et al., 1998), (Hall & Parmentier, 2003), and (Austin
 134 & Evans, 2007), were developed for solid earth studies and do not incorporate effects of
 135 migration recrystallization because rocks tend to deform at temperatures well below their
 136 melting temperatures. Ice on Earth is never more than a few tens of degrees colder than
 137 its melting temperature and thus deformation can warm ice to within a few degrees or
 138 less of its melting temperature (Meyer & Minchew, 2018), where we'd expect migration
 139 recrystallization to be most active.

140 Migration Recrystallization

141 The driving forces for migration recrystallization are the stress gradients created
 142 by heterogeneities in dislocation density that drive the outward migration of grain bound-
 143 aries (Figure 1) (Derby & Ashby, 1987). Once the strain energy of grains exceeds the
 144 surface energy of the grain boundaries of an individual grain, recrystallization begins in
 145 a wave from regions of high strain energy and large gradients in strain energy (Duval et
 146 al., 1983; R. Alley, 1992). The grain boundaries of an individual grain migrate outwards
 147 to reduce the lattice strain energy. Recrystallization ceases when the boundary energy
 148 of the grain exceeds the lattice strain energy of the grain (Duval & Castelnau, 1995).

149 In this study, we derive a steady-state model and thus we consider the bulk prop-
 150 erties of a macroscopic parcel of ice, rather than any localized discontinuities, when de-
 151 termining when migration recrystallization occurs. Since strain must be accumulated to

152 generate dislocations, previous studies have assumed that this criterion is fulfilled for strains
 153 larger than 1–10% (Duval & Castelnau, 1995). Strains of this magnitude are likely in
 154 shear margins of fast-flowing glaciers and we can expect that once ice has deformed suf-
 155 ficiently to warm the ice to -10°C , the ice has achieved strains of 1–10%. Thus, here
 156 we let temperature be a proxy for strain and assume migration recrystallization occurs
 157 for temperatures that exceed approximately -10°C , as suggested by previous works (Duval,
 158 1981; T. Jacka & Maccagnan, 1984; Duval & Castelnau, 1995).

159 The temperature dependence of recrystallization kinetics are represented by the
 160 activation energies. Previous studies have shown that at temperatures above -10°C , the
 161 kinetics of creep and grain growth change discontinuously due to the formation of pre-
 162 melt film and the proximity to the melting point (T. H. Jacka & Li Jun, 1994; Dash et
 163 al., 2006; Rempel & Meyer, 2019). Here, we set the temperature dependence of activa-
 164 tion energies for creep and grain growth accordingly, such that temperature plays a sig-
 165 nificant role in determining which creep mechanism is dominant.

166 Ice sheet-scale shear stresses drive deformation in lateral shear margins, which con-
 167 sequently increases the density of dislocations within grains (Figure 1). We can repre-
 168 sent the driving force of migration recrystallization as the difference of energy associated
 169 with a dislocation density ρ_d (defined as the number of dislocations per unit surface area)
 170 between neighboring grains, expressed as (Duval et al., 1983; Derby & Ashby, 1987; Derby,
 171 1992)

$$\Delta E_{dis} = \frac{1}{2} \mu b^2 \Delta \rho_d \quad (3)$$

172 where μ is the shear modulus and b is the magnitude of the Burger’s vector. We express
 173 the change in dislocation density as $\Delta \rho_d \approx (\frac{D}{d})^q \rho_d$, where q is an exponent to be de-
 174 fined, and D is the characteristic length scale over which we consider the change in dis-
 175 location density. This expression is physically justified by the fact that the length scale
 176 over which we consider changes in dislocation density is approximately the grain size d
 177 (Duval et al., 1983; R. Alley, 1992). The scaling of grain size by the characteristic length
 178 scale D gives us a term physically comparable to strain. We relate dislocation density
 179 to the applied shear stress τ_s as $\rho_d \approx \frac{\tau_s^2}{\mu^2 b^2}$. This relationship can be understood the-
 180 oretically by equating the internal stress from dislocation density ρ_d with the stress ap-
 181 plied to the material (R. Alley, 1992) and has been derived and applied in metals and
 182 ceramics studies (Duval et al., 1983).

183 Applying these expressions for the change in dislocation density and for disloca-
 184 tion density to Equation 3, we can find the change in energy associated with dislocation
 185 density, which is the driving force for migration recrystallization (F_{mig}):

$$F_{mig} = \Delta E_{dis} \approx \frac{1}{2} \left(\frac{D}{d} \right)^q \frac{\tau_s^2}{\mu} \quad (4)$$

186 We can find an expression for the change of grain size by considering the growth rate for
 187 grain boundary migration, which is equal to the velocity of migration, $v = M F_{mig}$, where
 188 M is the mobility of the grain boundary (Duval et al., 1983; Derby & Ashby, 1987; Derby,
 189 1992). The mobility of grain boundaries is expressed as $M = M_0 \exp \left[-\frac{Q_m}{RT} \right]$, where
 190 Q_m is the activation energy for grain boundary mobility, R is the ideal gas constant, T
 191 is temperature, and M_0 is the intrinsic mobility (Higashi, 1978), defined here as $M_0 =$
 192 $0.023 \text{ m}^4 \text{ J}^{-1} \text{ s}^{-1}$ (Llorens et al., 2017). The rate of change in internal strain energy due
 193 to migration recrystallization, \dot{E}_{mig} (Equation 5), is the time derivative of Equation 4,
 194 represented as

$$\dot{E}_{mig} = -\frac{1}{2} \frac{\tau_s^2}{\mu} q \frac{D^q}{d^{q+1}} \dot{d}_{mig} \quad (5)$$

$$\dot{d}_{mig} = MF_{mig} = \frac{1}{2} \frac{\tau_s^2}{\mu} \frac{D^q}{d^q} M \quad (6)$$

195 with the corresponding rate of change in grain size given by Equation 6.

196 Normal Grain Growth

197 The expression for the increase in grain size from normal grain growth is well-established
 198 and derived from the change in surface energy that occurs due to the migration of a grain
 199 boundary (R. Alley et al., 1986b):

$$d^p = d_0^p + kt \quad (7)$$

200 where p is the grain-growth exponent (to be constrained), d_0 is the initial grain size, and
 201 k is the grain growth rate factor. The grain growth factor is parameterized by $k = k_0 \exp \left[-\frac{Q_{gg}}{RT} \right]$,
 202 where k_0 is an empirical prefactor and Q_{gg} is the activation energy for normal grain growth
 203 (Duval, 1985; R. Alley et al., 1986b; T. H. Jacka & Li Jun, 1994). The rate of change
 204 in grain size due to normal grain growth \dot{d}_{nor} is the time-derivative of Equation 7.

205 Rotation Recrystallization

206 Rotation recrystallization is also well-studied and results in the subdivision of grains, which
 207 increases surface energy within a volume of a polycrystalline material (Duval & Castel-
 208 nau, 1995). This change in surface energy is related to a geometric constant that rep-
 209 represents the characteristic shape of grains, grain size, and grain boundary energy γ (R. Al-
 210 ley et al., 1986b; Austin & Evans, 2007). Grain boundary energy γ represents the change
 211 in free energy resultant from a change in area of the grain (Derby & Ashby, 1987), and
 212 laboratory experiments has found the value to be $\gamma = 0.065 \frac{\text{J}}{\text{m}^2}$ (Ketcham & Hobbs,
 213 1969). From this, the rate of change in internal energy density to rotation recrystalliza-
 214 tion is given as the change in surface energy, as shown in (Austin & Evans, 2007):

$$\dot{E}_{rot} = \frac{-c\gamma}{d^2} \dot{d}_{rot} \quad (8)$$

215 Steady-State Grain Size

216 Grain size evolution is a function of current grain size for all three recrystalliza-
 217 tion mechanisms. In the case of normal grain growth and migration recrystallization, the
 218 exponents p and q respectively govern the rate of grain growth. We note that both nor-
 219 mal grain growth and migration recrystallization occur by grain boundary migration. Since
 220 both recrystallization processes occur by the same process, with different driving forces,
 221 the change in grain size due to migration recrystallization and normal grain growth should
 222 have the same grain-size dependence. To represent this condition and to derive an ex-
 223 pression for the steady-state grain size, we thus assume $q = \frac{p}{2}$. We then define the ex-
 224 pression for steady-state grain size, accounting for the contribution of all mechanisms
 225 to grain size (Equation 1) and the mechanical work that goes into recrystallization (Equa-
 226 tion 2):

$$d_{ss} = \left[\frac{\overbrace{4kp^{-1}c\gamma\mu^2}^{\text{Normalgraingrowth}} + \overbrace{\tau_s^4 D^p \left(\frac{p}{2}\right) M}^{\text{Migrationrecrystallization}}}{\underbrace{8(1-\Theta)\tau_s\dot{\epsilon}_s\mu^2}_{\text{RotationRecrystallization}}} \right]^{\frac{1}{1+p}} \quad (9)$$

227 where $\dot{\epsilon}_s$ is the shear strain rate. The full derivation is found in Supplement Section A.
 228 The numerator consists of both grain growth mechanisms and the denominator describes
 229 the contribution of grain reduction, similar to relations derived previously (Derby & Ashby,
 230 1987). Without any clear estimates for Θ , we assume $\Theta \approx 1$, implying that most of the
 231 work done during deformation drives changes in thermal energy that warm the ice, a com-
 232 mon assumption made when studying shear margins of glaciers (Jacobson & Raymond,
 233 1998; Suckale et al., 2014; Perol & Rice, 2015; Meyer & Minchew, 2018; Haseloff et al.,
 234 2019; Hunter et al., 2021).

235 Model Validation

236 We use GRIP ice core temperature and grain size datasets (Gundestrup et al., 1993;
 237 Thorsteinsson et al., 1997; Johnsen et al., 1997) to benchmark our model due to the avail-
 238 ability of grain size and temperature data. We show in Supplement Section B that the
 239 model provides a good fit to both GISP2 ice core data and WAIS Divide ice core data
 240 as well, showing that the model is applicable to different ice sheets and different regions.
 241 The GRIP ice core is taken in a relatively stagnant region of the Greenland Ice Sheet
 242 and since we are primarily interested in grain sizes in rapidly deforming regions (shear
 243 margins of glaciers), the comparison here is solely to ensure our model parameterizes the
 244 physics underlying grain processes accurately.

245 The ice is frozen to the bed in the region from which the GRIP ice core was taken,
 246 and so both shear strain rate (computed from temperature and shear stress; Figure 2b)
 247 and observed temperature (Figure 2a) increase rapidly with depth near the bed. The re-
 248 gion of GRIP is near an ice divide, and therefore the shear strain rates and shear stresses
 249 in this region are orders of magnitude smaller than we would expect to find in shear mar-
 250 gins. The depth profile of strain rate and shear stress come from a nonzero surface slope
 251 α , which drives ice deformation. We compute stresses and strain rates for $\alpha = 0.01^\circ$
 252 and $\alpha = 0.05^\circ$, reasonable values for the surface slope in the region of the GRIP ice core
 253 (Helm et al., 2014). The grey shading represents the depth at which the ice has not yet
 254 reached steady state (dark grey for $\alpha = 0.05^\circ$, light grey for $\alpha = 0.01^\circ$), and there-
 255 fore the models should not predict the correct grain sizes. Since the fit near the bed does
 256 not significantly depend on the grain sizes estimated more than a few hundred meters
 257 above where the ice reaches the critical temperature, the regions not at steady state are
 258 unlikely to affect the grain sizes at depth.

259 Our model is largely consistent with the grain size data from the GRIP ice core (Fig-
 260 ure 2c). Near the bed, migration recrystallization is the dominant mechanism and thus
 261 responsible for the rapid increase in grain size. When applying our model, which incor-
 262 porates the contributions of migration recrystallization, we see a reasonable fit to the
 263 GRIP ice core data near the bed. The depth at which grains begin to grow is largely dic-
 264 tated by temperature. At temperatures of approximately $-10^\circ C$, grain boundaries be-
 265 come more mobile, enabling high-velocity grain boundary migration (Duval & Castel-
 266 nau, 1995; Urai et al., 1995; Montagnat & Duval, 2000). This critical temperature T_c
 267 at which this change in activation energy occurs has been experimentally determined.
 268 However, studies have shown that critical temperatures between $-8^\circ C$ and $-15^\circ C$ may
 269 apply to natural conditions (Barnes et al., 1971; D. L. Goldsby & Kohlstedt, 2001; Kuiper
 270 et al., 2020). We show model estimates of grain size for a critical temperature of $T_c =$
 271 $-13^\circ C$ (Figure 2), to demonstrate that defining a critical temperature within reason-

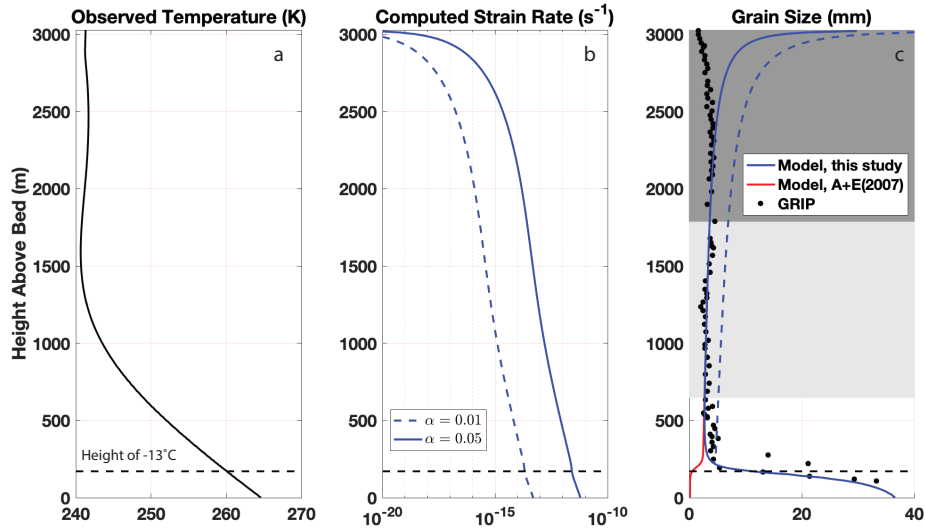


Figure 2. Results of a steady-state grain size model: (a) Temperature measured from the GRIP ice core, (b) strain rate computed from shear stress using the constitutive relation (Glen’s Flow Law) for ice (where the flow-rate parameter is found from temperature by the Arrhenius relation and the flow-law exponent is taken to be $n = 3$ (Jezek et al., 1985; K. Cuffey & Paterson, 2010) for surface slopes of 0.05° (solid line) and 0.01° (dashed line), (c) grain size computed from the model presented in this study from surface slopes of 0.05° (solid blue line) and 0.01° (dashed blue line), reasonable surface slopes for this region (Helm et al., 2014), the model presented in (Austin & Evans, 2007) (red line), and measured from the GRIP ice core (black circles). The grey shading represents the depths at which the ice has not yet reached steady-state (dark grey for a surface slope of 0.05° and light grey for a surface slope of 0.01°) and may be contaminated by firn processes. For shear margins, the most relevant areas are those that are in steady state and thus outside the grey shaded boxes (discussed further in Supplement Section D).

272 able bounds of the canonical value of -10°C produces an accurate estimate of the grain
 273 size profile. However, for the remainder of this study, we use the canonical value $T_c =$
 274 -10°C for consistency with much of the salient literature referenced here.

275 The magnitude of the change in grain size with depth is controlled primarily by
 276 two parameters: the characteristic length-scale D and the grain growth exponent p (Equa-
 277 tion 7). These two parameters are poorly constrained in natural deforming glacier ice.
 278 Traditionally, the grain growth exponent is taken to be $p = 2$ in glacier ice, from a fit
 279 to laboratory data and borehole measurements (Duval, 1985; R. Alley et al., 1986b, 1986a).
 280 Recent work has shown that this value of the grain growth exponent best fits bubble-
 281 free glacier ice and that bubbled ice more likely has a higher grain growth exponent (Azuma
 282 et al., 2012). Since GRIP ice core is in a slowly-deforming region that is likely to have
 283 a higher concentration of bubbles, we use $p = 9$ for that fit. On the other hand, we are
 284 interested in rapidly-deforming regions that likely have a low concentration of bubbles,
 285 so we use $p = 2$ for the remainder of this study. We reserve for future work a complete
 286 exploration of the effect of varying grain growth exponents. The characteristic grain size
 287 D is uncertain as well, given that this is a scaling factor and the average grain size can
 288 vary widely in different parts of Antarctica. In the Supplement Section C, we show that
 289 values of D between 50 mm and 100 mm best represent the ice core data we use here,
 290 and we take $D = 50$ mm to approximate the best fit.

291 Model Results in Shear Margins

292 We first apply this model to a single column of an idealized shear margin in which
 293 the strain rate is constant with depth. We compute grain size from three different strain
 294 rates, representing a reasonable range of strain rates seen in shear margins of Antarc-
 295 tic ice streams (K. E. Alley et al., 2018). We compute ice temperature from strain rate
 296 using the thermomechanical model developed by (Meyer & Minchew, 2018) (Figure 3b)
 297 (with vertical accumulation accounted for in the Peclet number, where $\text{Pe} = 2$).

298 For a low strain rate ($\dot{\epsilon} = 6 \times 10^{-10} \text{ s}^{-1}$), temperature increases only slightly with
 299 depth and thus grain size remains relatively constant with depth. For an intermediate
 300 strain rate ($\dot{\epsilon} = 1.3 \times 10^{-9} \text{ s}^{-1}$), comparable to that found in shear margins of most
 301 ice streams in Antarctica, temperature increases significantly with depth, reaching the
 302 melting temperature approximately 100 m from the bed. Grains grow with depth un-
 303 til the critical temperature of -10°C , where there is a decrease in grain sizes due to an
 304 increase in the prevalence of rotation recrystallization. There is then a rapid growth of
 305 grains due to temperatures approaching -10°C , when enough strain energy has built
 306 for grain boundaries to migrate through migration recrystallization. Below approximately
 307 500 meters above the bed, grain sizes become roughly constant with depth due to strain
 308 rate and temperature increasing enough such that creep and subsequent grain reduction
 309 due to rotation recrystallization becomes more active and balances the contribution of
 310 migration recrystallization. For a high strain rate ($\dot{\epsilon} = 6 \times 10^{-8} \text{ s}^{-1}$), temperatures
 311 increase dramatically, reaching the melting point approximately 700 m above the bed.
 312 The ice remains temperate for the remainder of the ice column. Due to the dramatic in-
 313 crease in temperature in the first few hundred meters, grain size increases from ~ 2 mm
 314 at the surface to ~ 13 mm approximately 200 m from the surface. Grain sizes then re-
 315 main roughly constant with depth for the remainder of the ice column. The estimate that
 316 grains are large in shear margins and regions where the ice is warm is supported by ob-
 317 servations from Antarctic ice streams (Jackson & Kamb, 1997) and from temperate glaciers
 318 (Tison & Hubbard, 2000).

319 In contrast to our results, studies in the solid earth community have considered the
 320 effect of recrystallization on grain sizes in shear zones and found that grain size reduces
 321 in shear zones due to the dominance of rotation recrystallization in regions with high strain
 322 rate (Karato et al., 1980; J. H. P. De Bresser et al., 1998; J. De Bresser et al., 2001; Montési

323 & Hirth, 2003). Rocks deform far below their melting temperature, so a temperature in-
 324 crease by shear heating would have to be much larger than that for ice, which deforms
 325 close to its melting temperature. Ice temperatures near the melting point drives migra-
 326 tion recrystallization, which results in a growth in grains in shear margins rather than
 327 a reduction in grain size.

328 **Effect of Grain Size on Ice Rheology**

329 Grain size affects the rheology of ice. Typically, ice rheology is described through
 330 a power-law relationship (Glen’s flow law), which relates strain rate to stress raised to
 331 a power n , $\dot{\epsilon} = A\tau^n$. The value of n reflects the creep mechanism that ice deforms by
 332 and thus the choice of n in ice-flow modeling significantly affects the behavior of deform-
 333 ing ice. Uncertainties in the parameters of this flow law contribute significantly to un-
 334 certainties in large-scale ice-flow modeling (Zeitze et al., 2020), and constraining values
 335 of n is critical to making projections of ice sheet behavior.

336 Values of $n = 3$ are commonly used because this value fits laboratory data for the
 337 creep of ice (Jezek et al., 1985). However, a value of $n = 3$ does not clearly match with
 338 one creep mechanism. Instead, a flow law exponent of $n \approx 3$ may describe creep by a
 339 combination of dislocation creep ($n \approx 4$), which is grain-size-independent, and grain-
 340 boundary sliding ($n \approx 2$), which is grain-size-dependent (D. Goldsby & Kohlstedt, 1997;
 341 Montagnat & Duval, 2000; D. L. Goldsby & Kohlstedt, 2001; Behn et al., 2020). Deform-
 342 ation of ice with large grain sizes generally favors dislocation creep as the dominant
 343 deformation mechanism.

344 Dislocation creep occurs through dislocations, line defects in the ice, which enable
 345 planes of the ice crystalline lattice to move past each other. Migration recrystallization
 346 annihilates dislocations through the migration of grain boundaries, further increasing grain
 347 size and producing space for new dislocations to move through, which allows for contin-
 348 ued dislocation creep. The rate of creep for grain-size-dependent deformation mechanisms
 349 (all except dislocation creep) is inversely related to grain size, so in ice with large grains,
 350 the rate of grain-size-dependent creep is likely to be low. Thus, as grains grow, the flow
 351 law tends to a power-law relationship with $n = 4$, describing dislocation creep as the
 352 sole creep mechanism.

353 This suggests that in areas of rapid deformation, such as the margins of ice streams,
 354 modeling ice flow with a flow-law exponent of $n \approx 4$ (dislocation-creep-dominant flow)
 355 may more accurately capture the dynamics occurring as the ice deforms, a result also
 356 estimated using satellite observations of ice shelves (Millstein & Minchew, 2020). In Sup-
 357 plement Section C, we show these results from our model for varying values of n . The
 358 value of n directly affects the rate of flow of ice, as viscosity scales with strain rate to
 359 the power of $\frac{1-n}{n}$. Thus, a value of $n = 4$ implies a lower viscosity for a given strain
 360 rate, suggesting that models may be overestimating the viscosity of ice in areas of rapid
 361 deformation.

362 **Effect of grain size on fracture vulnerability**

363 In the absence of pre-existing macro-scale fractures, the size of grains has a signif-
 364 icant effect upon the strength of ice because grain boundaries are themselves flaws in the
 365 ice along which cracks can propagate (Schulson & Hibler, 1991). Therefore, . Intuitively,
 366 an increase in grain size translates to an increase in the length of grain boundaries, re-
 367 sulting in an increase in vulnerability to fracture (Figure 3a). Laboratory studies have
 368 similarly found that the tensile strength of ice σ_t , defined as the total stress required to
 369 fracture ice in tension, decreases with increasing grain size according to the following re-
 370 lationship: (Currier & Schulson, 1982; Schulson et al., 1984; W. A. Nixon & Schulson,
 371 1988)

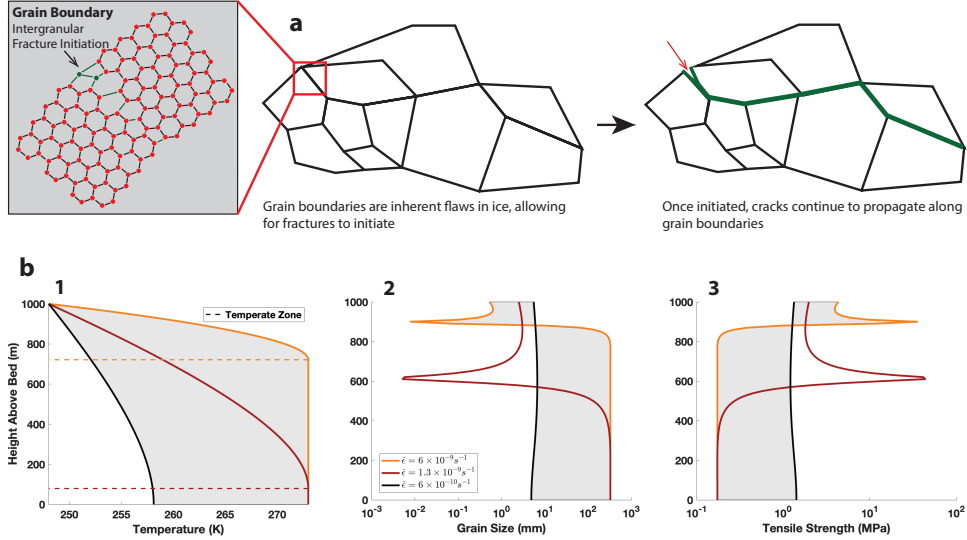


Figure 3. (a) Schematic that illustrates the role grain boundaries play in fracture. This shows a theoretical polycrystalline ice of 10 grains. Grain boundaries are inherent flaws in the ice because they interrupt the ordered structure of the lattice (inset). This enables initiation of intergranular fracture in response to stresses. Once the fracture is initiated, cracks propagate along grain boundaries because they are the weakest part of the ice. Outlined in green is a potential path a fracture may take. (b) Results from an idealized model showing the relationship between ice temperature, grain size, and tensile strength. First panel: Ice temperature computed from the thermomechanical model presented in (Meyer & Minchew, 2018), Second panel: Grain size computed from the steady-state grain size model developed here (Equation 9), Third panel: Tensile strength computed from Equation 10, for 3 strain rates.

$$\sigma_t = K d^{-\frac{1}{2}} \quad (10)$$

372 where K is a constant. While this is an empirical relationship, studies have developed
 373 theoretical bases for this relationship. The most prevalent explanation is the dislocation
 374 pileup mechanism, which explains deformation through the pileup of dislocations at the
 375 edge of a grain that then induces deformation in a neighboring grain (Li & Chou, 1970).
 376 Fractures initiate to reduce the stress that forms due to this dislocation pileup. The stress
 377 required for this to occur has the same grain size dependence as that in Equation 10 Li1970,
 378 Schulson1984, Cole1987.

379 We apply Equation 10 to compute the tensile strength of ice as a function of grain
 380 size (setting $K = 0.052 \text{ MPa m}^{\frac{1}{2}}$ (Lee & Schulson, 1988)) for the case of the idealized
 381 shear margin (Figure 3b). For a low strain rate, since grain sizes remain approximately
 382 constant with depth, tensile strength also remains roughly constant with depth and $\sigma_t \approx$
 383 1.2 MPa. For an intermediate strain rate, grain sizes grow between approximately 400
 384 and 600 m above the bed before reaching a steady-state grain size of approximately 15
 385 mm and then remaining constant with depth for the remainder of the ice column. Simi-
 386 larly, tensile strength remains constant until approximately 600 m above the bed. At
 387 this depth, tensile strength increases sharply due to a decrease in grain size, and then
 388 tensile strength decreases to approximately 0.4 MPa and remains constant with depth
 389 to the bed. At a high strain rate, tensile strength follows a similar pattern as that for

intermediate strain rates, though the decrease in tensile strength occurs closer to the surface (~ 900 m height).

In locations of ice sheets in which the ice is frozen to the bed, a similar decrease in tensile strength will be likely near the bed due to an increase in grain size caused by migration recrystallization, as seen in the GRIP ice core (Figure 2). However, that decrease in tensile strength would be coupled with an increase in the overburden pressure, preventing tensile fractures from forming. In the case of shear margins, however, we observe a decrease in tensile strength to approximately 25% of the tensile strength a few hundreds of meters below the surface. With relatively low overburden pressure at these depths, this leaves a significant depth of the shear margin vulnerable to the propagation of microcracks along grain boundaries and thus the nucleation of large-scale fractures. Though not explicitly represented in these models, we would expect the water pressure at the base of ice shelves to facilitate the opening of tensile fractures, which renders the deeper portions of the shear margins on ice shelves, where tensile strength is lowest, quite vulnerable to fracture.

Application to Pine Island Glacier, West Antarctica

We apply our model to Pine Island Glacier in West Antarctica because of its rapid deformation and potential for large-scale implications for the Antarctic Ice Sheet (Rignot et al., 2002; Wingham et al., 2009; Joughin et al., 2014). The yearly velocity of Pine Island Glacier is found from LANDSAT 8 satellite imagery (Figure 4b) (Gardner et al., 2018), ice thickness is calculated from basal topography from BedMachine (Morlighem et al., 2020), and surface elevation from the Reference Elevation Model of Antarctica (Howat et al., 2019). We use surface mass balance, averaged over the years 1979-2019, from the RACMO model of Antarctica to set the rate of vertical advection in the thermomechanical model (Van Wessem et al., 2014). Results for other outlet glaciers in Antarctica are shown in Supplement Section F.

We compute grain size from surface strain rates (calculated from surface velocity; Figure 4b), ice temperature (calculated from surface strain rates), and ice thickness. Grain size is also dependent upon Θ , the fraction of work dissipated as heat. Commonly, it is assumed that all the work done during deformation is dissipated as heat, $\Theta \approx 1$ (Suckale et al., 2014; Perol & Rice, 2015; Hewitt & Schoof, 2017). However, the value has not been experimentally or theoretically constrained. Here, we present results for $\Theta \approx 1$ and in the Supplement Section F we present results with $\Theta = 0.5$ and $\Theta = 0.25$. The tensile strength of ice is then computed from grain size. We show three slices of the ice column: the grain size and tensile strength at 25% of the ice thickness, at 50% of the ice thickness, and 75% of the ice thickness (Figure 4c).

Grains are large in the shear margins of Pine Island Glacier (~ 15 mm) relative to the rest of the glacier and ice core data. This is likely due to high strain rates resulting in elevated ice temperatures (at or near the melting point). Previous studies show extensive zones of temperate ice in the shear margins of Pine Island Glacier (Meyer & Minchew, 2018), and this drives migration recrystallization and increases the size of grains. The depth profile largely mirrors that seen in the idealized case (Figure 3b): at the bed, most of the margin contains coarse-grained ice. A similar area of coarse-grained ice exists at 25% of the ice thickness. In the middle of the ice column (50%), the area of coarse-grained ice thins but still spans a significant portion of the margin, especially upstream. Finally, near the surface (75% of ice thickness), the area of large grains thins even more but still dominates the shear margin (Figure 4c,d). The difference between grain size in the margins and grain size in the trunk of the ice stream decreases as Θ decreases (as less work is dissipated as heat). Even at low Θ , grains are still larger in the margins (Supplement Section F). This may imply that, in the margins, dislocation creep is the dom-

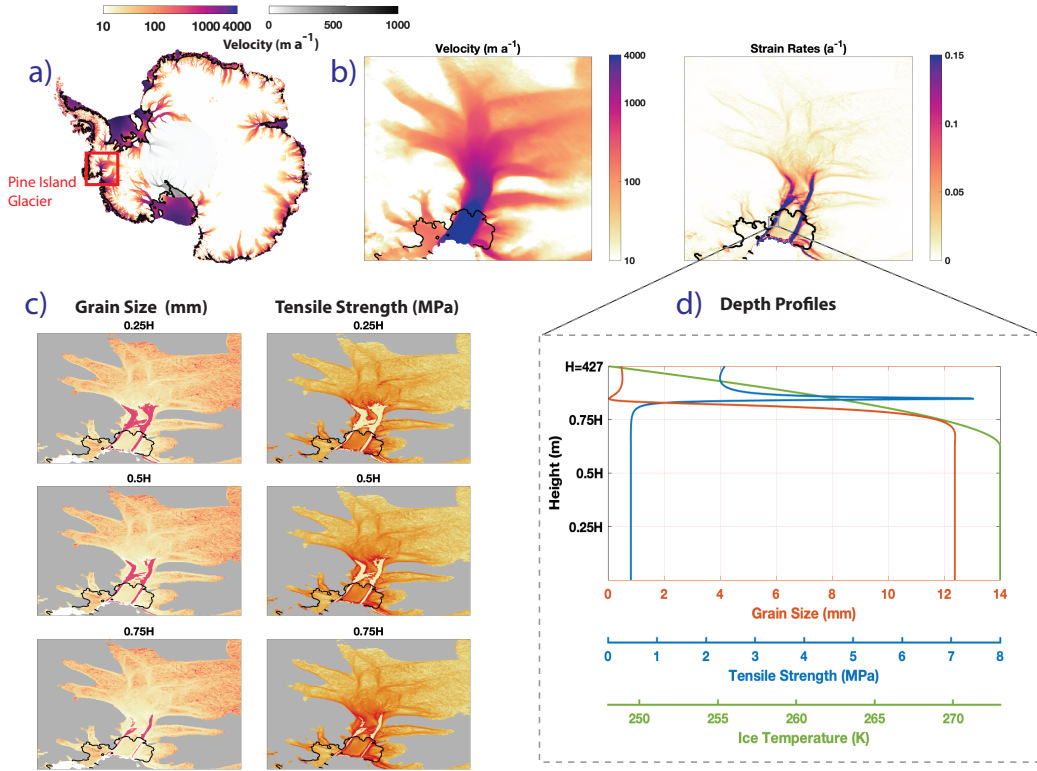


Figure 4. (a) Surface velocity of Antarctica from Landsat 7 and 8 (Gardner et al., 2018), with the pole hole filled in from NASA MEaSUREs (Rignot et al., 2011; Mouginot et al., 2012; Rignot et al., 2017), with the region of Pine Island Glacier outlined in red. (b) Surface velocity and surface strain-rates of Pine Island Glacier. (c) Estimated grain sizes and tensile strength at varying depths: 25% of ice thickness (H) from the bed, 50% of ice thickness from the bed, and 75% of ice thickness from the bed. Areas where the model is not valid (flow speed $< 30 \text{ m a}^{-1}$) are shown in grey. Here we show results for $\Theta \approx 1$, the assumption used in thermomechanical models of ice (Hewitt & Schoof, 2017). Results using other values of Θ are shown in Supplement Section F. (d) Depth profiles of grain size, tensile strength, and ice temperature for a single point of the shear margin of the Pine Island Glacier ice shelf.

inant deformation mechanism and thus modeling the evolution of Pine Island Glacier using $n = 4$ in the margins is most accurate.

Large grain sizes in the margins translate to relatively low values of tensile strength. Tensile strength drops from ~ 1.5 MPa in the fine-grained regions to ~ 0.2 MPa in the coarse-grained regions. These values are significantly lower than some estimated tensile strength values for relatively pristine and large undeformed (Ultee et al., 2020) and within the range of reasonable values found by other studies (Vaughan, 1993). Furthermore, there is a significant portion of the shear margin that has very low tensile strength near the surface (75% of ice thickness). A reduction in tensile strength occurs for low values of Θ as well, though the reduction is not as significant and does not extend as far up the ice column (Supplement Section F). This dramatic drop in tensile strength, particularly near the surface, may increase the vulnerability of the shear margin to fracture and is positioned approximately where significant damage and fracturing in Pine Island Glacier have been observed (Lhermitte et al., 2020). Ice shelves are particularly vulnerable to changes in tensile strength because basal crevasses are more easily formed than in grounded ice due to the fact that the cracks are water-filled. A reduction in the strength of ice at the base of the ice column may increase the vulnerability of ice shelves significantly relative to grounded ice since it allows for cracks to propagate from the base of the ice shelf and may allow for full-thickness fractures to develop. This drop in tensile strength is due to the rate of deformation in shear margins, and so as Pine Island Glacier accelerates in a changing climate, the ice shelf of Pine Island Glacier may become more vulnerable to fracture and calving events (Rignot et al., 2002; Joughin et al., 2003).

Conclusions

In this study, we show that grain sizes in shear margins are large, which influences the rate of creep and vulnerability to fracture of the ice and may contribute to accelerated flow and instability of ice shelves. To show this, we derive a new model for migration recrystallization, a mechanism for recrystallization that is dominant at high strain rate and high temperature and results in an increase in grain size. Our model demonstrates that migration recrystallization is dominant in shear margins and thus ice grains in shear margins are large (~ 15 mm), compared to grain sizes of $\sim 2 - 7$ mm in surrounding regions. This is a significant deviation from previous work in solid earth recrystallization studies that have shown shear zones of rock to be fine-grained. This distinction arises because ice in terrestrial glaciers and ice sheets is close to its melting temperature and thus migration recrystallization can outpace rotation recrystallization resulting in coarse grains in shear zones. We show here that this result may have implications for the vulnerability of shear margins to fracture and the rheology of ice in shear margins.

The flow of ice is described by a constitutive relation that relates strain rate and stress through a power law, with a flow exponent n . The value of $n = 3$ has been found to match laboratory data and is commonly used in ice sheet and ice flow models. However, we suggest here that in shear margins where grain sizes are large, dislocation creep ($n = 4$) is likely to be the dominant deformation mechanism, since large grain sizes give more area for slip to occur through dislocations and large grain sizes also reduce the rates of creep by mechanisms such as grain-boundary sliding and diffusion creep. Thus, a flow law exponent of $n \approx 4$ may be more appropriate than the commonly-used $n = 3$ for rapidly-deforming regions of ice streams, such as the lateral margins. This may imply that, by using the traditional Glen's flow law with $n = 3$ in large-scale ice flow models, we are underestimating the rate of creep, and consequently the acceleration of flow, in key regions of Antarctica. While we do not directly model the effects of dynamic recrystallization on fabric development here, including fabric is likely to strengthen this result due to the creation of a single-maximum fabric that softens the ice and allows for higher rates of deformation. Further, it is well known that an increase in grain size re-

492 duces the strength of polycrystalline materials. Here, we show that the tensile strength
 493 of ice in shear margins of Pine Island Glacier, West Antarctica are approximately 25%
 494 of the tensile strength of ice in the centerline of the glacier. This decrease in tensile strength
 495 may give rise to damage and fracture that previous studies have identified in Pine Is-
 496 land Glacier (Lhermitte et al., 2020). Further, this model produces predictions of grain
 497 size that can be tested by observations of grain size in shear margins.

498 This new understanding of recrystallization in shear zones may provide a way to
 499 estimate more accurately the vulnerability of rapidly deforming glaciers to instability by
 500 parameterizing the effect of dynamic recrystallization processes in large-scale ice flow mod-
 501 els. This work provides inroads into thinking about how to represent different types of
 502 flow in large-scale ice flow models with a spatially varying flow exponent n . Finally, this
 503 work suggests that dynamic recrystallization processes significantly affect the physical
 504 properties and dynamics of rapidly-deforming glaciers, and further work will consider
 505 the role that dynamic recrystallization and grain-scale processes play in the large-scale
 506 dynamics and energetics of shear margins.

507 Acknowledgments

508 We acknowledge enlightening conversations and feedback from Maurine Montagnat, Brian
 509 Evans, and Mark Behn, along with feedback from the MIT Glaciers Group. M.I.R. grate-
 510 fully acknowledges funding from the Martin Fellowship and the Sven Treitel Fellowship.
 511 B.M. acknowledges funding from two NSF-NERC grants, award numbers 1739031 and
 512 1853918, and a grant from the NEC Corporation Fund for Research in Computers and
 513 Computation. No new data were produced for this study, and data used in this study
 514 are publicly available through their respective publications, cited here. The code for the
 515 model and that generates the figures in this paper can be found at: [https://github.com/
 516 megr090/grain-size-tensile-strength-model](https://github.com/megr090/grain-size-tensile-strength-model).

517 References

- 518 Alley, K. E., Scambos, T. A., Anderson, R. S., Rajaram, H., Pope, A., & Haran,
 519 T. M. (2018). Continent-wide estimates of Antarctic strain rates from Land-
 520 sat 8-derived velocity grids. *Journal of Glaciology*, *64*(244), 321–332. doi:
 521 10.1017/jog.2018.23
- 522 Alley, R. (1988, apr). Fabrics in Polar Ice Sheets: Development and Prediction.
 523 *Science*, *240*(4851), 493–495. Retrieved from [https://www.sciencemag.org/
 524 lookup/doi/10.1126/science.240.4851.493](https://www.sciencemag.org/lookup/doi/10.1126/science.240.4851.493) doi: 10.1126/science.240.4851
 525 .493
- 526 Alley, R. (1992, jan). Flow-law hypotheses for ice-sheet modeling. *Journal of
 527 Glaciology*, *38*(129), 245–256. Retrieved from [https://www.cambridge.org/
 528 core/product/identifier/S0022143000003658/type/journal%7B%7Darticle](https://www.cambridge.org/core/product/identifier/S0022143000003658/type/journal%7B%7Darticle)
 529 doi: 10.3189/S0022143000003658
- 530 Alley, R., Perepezko, J., & Bentley, C. (1986a, jan). Grain Growth in Po-
 531 lar Ice: II. Application. *Journal of Glaciology*, *32*(112), 425–433. Re-
 532 trieved from [https://www.cambridge.org/core/product/identifier/
 533 S0022143000012132/type/journal%7B%7Darticle](https://www.cambridge.org/core/product/identifier/S0022143000012132/type/journal%7B%7Darticle) doi: 10.3189/
 534 S0022143000012132
- 535 Alley, R., Perepezko, J., & Bentley, C. (1986b). Grain Growth in Polar Ice:
 536 I. Theory. *Journal of Glaciology*, *32*(112), 425–433. doi: 10.3189/
 537 s0022143000012132
- 538 Austin, N. J., & Evans, B. (2007). Paleowattmeters: A scaling relation for dynam-
 539 ically recrystallized grain size. *Geology*, *35*(4), 343. Retrieved from [https://
 540 pubs.geoscienceworld.org/geology/article/35/4/343-346/129818](https://pubs.geoscienceworld.org/geology/article/35/4/343-346/129818) doi:
 541 10.1130/G23244A.1
- 542 Azuma, N., Miyakoshi, T., Yokoyama, S., & Takata, M. (2012, sep). Impeding effect

- 543 of air bubbles on normal grain growth of ice. *Journal of Structural Geology*,
 544 42, 184–193. Retrieved from <http://dx.doi.org/10.1016/j.jsg.2012.05>
 545 .005<https://linkinghub.elsevier.com/retrieve/pii/S019181411200123X>
 546 doi: 10.1016/j.jsg.2012.05.005
- 547 Barnes, P., Tabor, D., & Walker, J. C. F. (1971, aug). The friction and creep
 548 of polycrystalline ice. *Proceedings of the Royal Society of London. A.*
 549 *Mathematical and Physical Sciences*, 324(1557), 127–155. Retrieved from
 550 <https://royalsocietypublishing.org/doi/10.1098/rspa.1971.0132> doi:
 551 10.1098/rspa.1971.0132
- 552 Behn, M. D., Goldsby, D. L., & Hirth, G. (2020). The role of grain-size evolu-
 553 tion on the rheology of ice: Implications for reconciling laboratory creep data
 554 and the Glen flow law. *The Cryosphere Discussions*(November), 1–31. Re-
 555 trieved from <https://tc.copernicus.org/preprints/tc-2020-295/> doi:
 556 10.5194/tc-2020-295
- 557 Clerc, F., Minchew, B. M., & Behn, M. D. (2019). Marine Ice Cliff Instability Mit-
 558 igated by Slow Removal of Ice Shelves. *Geophysical Research Letters*, 46(21),
 559 12108–12116. doi: 10.1029/2019GL084183
- 560 Cuffey, K., & Paterson, W. (2010). *The Physics of Glaciers* (Fourth ed.). Elsevier.
- 561 Cuffey, K. M., Thorsteinsson, T., & Waddington, E. D. (2000, dec). A renewed ar-
 562 gument for crystal size control of ice sheet strain rates. *Journal of Geophysi-
 563 cal Research: Solid Earth*, 105(B12), 27889–27894. Retrieved from <http://doi>
 564 .wiley.com/10.1029/2000JB900270 doi: 10.1029/2000JB900270
- 565 Currier, J., & Schulson, E. (1982, aug). The tensile strength of ice as a function
 566 of grain size. *Acta Metallurgica*, 30(8), 1511–1514. Retrieved from <https://>
 567 <linkinghub.elsevier.com/retrieve/pii/0001616082901717> doi: 10.1016/
 568 0001-6160(82)90171-7
- 569 Dash, J. G., Rempel, A. W., & Wettlaufer, J. S. (2006). The physics of premelted
 570 ice and its geophysical consequences. *Reviews of Modern Physics*, 78(3), 695–
 571 741. doi: 10.1103/RevModPhys.78.695
- 572 De Bresser, J., Ter Heege, J., & Spiers, C. (2001, may). Grain size reduction by dy-
 573 namic recrystallization: can it result in major rheological weakening? *Interna-
 574 tional Journal of Earth Sciences*, 90(1), 28–45. Retrieved from <http://link>
 575 .springer.com/10.1007/s005310000149 doi: 10.1007/s005310000149
- 576 De Bresser, J. H. P., Peach, C. J., Reijs, J. P. J., & Spiers, C. J. (1998, sep). On
 577 dynamic recrystallization during solid state flow: Effects of stress and tem-
 578 perature. *Geophysical Research Letters*, 25(18), 3457–3460. Retrieved from
 579 <http://doi.wiley.com/10.1029/98GL02690> doi: 10.1029/98GL02690
- 580 Derby, B. (1992, dec). Dynamic recrystallisation: The steady state grain size.
 581 *Scripta Metallurgica et Materialia*, 27(11), 1581–1585. Retrieved from
 582 <https://linkinghub.elsevier.com/retrieve/pii/0956716X92901488>
 583 doi: 10.1016/0956-716X(92)90148-8
- 584 Derby, B., & Ashby, M. (1987, jun). On dynamic recrystallisation. *Scripta Metal-
 585 lurgica*, 21(6), 879–884. Retrieved from <https://linkinghub.elsevier.com/>
 586 <retrieve/pii/0036974887903413> doi: 10.1016/0036-9748(87)90341-3
- 587 Duval, P. (1981). Creep and Fabrics of Polycrystalline Ice Under Shear and Com-
 588 pression. *Journal of Glaciology*, 27(95), 129–140.
- 589 Duval, P. (1985). Grain growth and mechanical behaviour of polar ice. *Annals of
 590 Glaciology*, 3–6.
- 591 Duval, P., Ashby, M. F., & Anderman, I. (1983). Rate-controlling processes in the
 592 creep of polycrystalline ice. *Journal of Physical Chemistry*, 87(21), 4066–4074.
 593 doi: 10.1021/j100244a014
- 594 Duval, P., & Castelnaud, O. (1995). Dynamic recrystallization of ice in polar ice
 595 sheets. *Journal de Physique IV*, 5(C3), 197–205. Retrieved from <http://www>
 596 .scopus.com/inward/record.url?eid=2-s2.0-33750590172{\&}partnerID=
 597 MN8TOARS doi: 10.1051/jp4

- 598 Duval, P., & Gac, H. L. (1980). Does the Permanent Creep-Rate of Polycrystalline
599 Ice Increase with Crystal Size? *Journal of Glaciology*, 25(91), 151–158. doi: 10
600 .3189/s0022143000010364
- 601 Duval, P., Montagnat, M., Grennerat, F., Weiss, J., Meyssonier, J., & Philip, A.
602 (2010, sep). Creep and plasticity of glacier ice: a material science perspec-
603 tive. *Journal of Glaciology*, 56(200), 1059–1068. Retrieved from [https://](https://www.cambridge.org/core/product/identifier/S0022143000213269/type/journal-article)
604 [www.cambridge.org/core/product/identifier/S0022143000213269/type/](https://www.cambridge.org/core/product/identifier/S0022143000213269/type/journal-article)
605 [journal-article](https://www.cambridge.org/core/product/identifier/S0022143000213269/type/journal-article) doi: 10.3189/002214311796406185
- 606 Gardner, A. S., Moholdt, G., Scambos, T., Fahnestock, M., Ligtenberg, S., van den
607 Broeke, M., & Nilsson, J. (2018, feb). Increased West Antarctic and unchanged
608 East Antarctic ice discharge over the last 7 years. *The Cryosphere*, 12(2), 521–
609 547. Retrieved from <https://tc.copernicus.org/articles/12/521/2018/>
610 doi: 10.5194/tc-12-521-2018
- 611 Goldsby, D., & Kohlstedt, D. (1997, nov). Grain boundary sliding in fine-
612 grained Ice I. *Scripta Materialia*, 37(9), 1399–1406. Retrieved from
613 <https://linkinghub.elsevier.com/retrieve/pii/S1359646297002467>
614 doi: 10.1016/S1359-6462(97)00246-7
- 615 Goldsby, D. L., & Kohlstedt, D. L. (2001, jun). Superplastic deformation of ice:
616 Experimental observations. *Journal of Geophysical Research: Solid Earth*,
617 106(B6), 11017–11030. Retrieved from [http://doi.wiley.com/10.1029/](http://doi.wiley.com/10.1029/2000JB900336)
618 2000JB900336 doi: 10.1029/2000JB900336
- 619 Gow, A. J., Meese, D. A., Alley, R. B., Fitzpatrick, J. J., Anandkrishnan, S.,
620 Woods, G. A., & Elder, B. C. (1997, nov). Physical and structural prop-
621 erties of the Greenland Ice Sheet Project 2 ice core: A review. *Journal*
622 *of Geophysical Research: Oceans*, 102(C12), 26559–26575. Retrieved from
623 <http://doi.wiley.com/10.1029/97JC00165> doi: 10.1029/97JC00165
- 624 Gudmundsson, G. H., Paolo, F. S., Adusumilli, S., & Fricker, H. A. (2019,
625 dec). Instantaneous Antarctic ice sheet mass loss driven by thinning ice
626 shelves. *Geophysical Research Letters*, 46(23), 13903–13909. Retrieved from
627 <https://onlinelibrary.wiley.com/doi/abs/10.1029/2019GL085027> doi:
628 10.1029/2019GL085027
- 629 Gundestrup, N., Dahl-Jensen, D., Johnsen, S., & Rossi, A. (1993, jul). Bore-hole
630 survey at dome GRIP 1991. *Cold Regions Science and Technology*, 21(4),
631 399–402. Retrieved from [https://linkinghub.elsevier.com/retrieve/pii/](https://linkinghub.elsevier.com/retrieve/pii/0165232X9390015Z)
632 0165232X9390015Z doi: 10.1016/0165-232X(93)90015-Z
- 633 Hall, C. E., & Parmentier, E. M. (2003, mar). Influence of grain size evolution
634 on convective instability. *Geochemistry, Geophysics, Geosystems*, 4(3). Re-
635 trieved from <http://doi.wiley.com/10.1029/2002GC000308> doi: 10.1029/
636 2002GC000308
- 637 Haseloff, M., Hewitt, I. J., & Katz, R. F. (2019, nov). Englacial Pore Water Local-
638 izes Shear in Temperate Ice Stream Margins. *Journal of Geophysical Research:*
639 *Earth Surface*, 124(11), 2521–2541. Retrieved from [https://onlinelibrary](https://onlinelibrary.wiley.com/doi/abs/10.1029/2019JF005399)
640 [.wiley.com/doi/abs/10.1029/2019JF005399](https://onlinelibrary.wiley.com/doi/abs/10.1029/2019JF005399) doi: 10.1029/2019JF005399
- 641 Helm, V., Humbert, A., & Miller, H. (2014, aug). Elevation and elevation change
642 of Greenland and Antarctica derived from CryoSat-2. *The Cryosphere*, 8(4),
643 1539–1559. Retrieved from [https://tc.copernicus.org/articles/8/1539/](https://tc.copernicus.org/articles/8/1539/2014/)
644 2014/ doi: 10.5194/tc-8-1539-2014
- 645 Hewitt, I. J., & Schoof, C. (2017, feb). Models for polythermal ice sheets and
646 glaciers. *The Cryosphere*, 11(1), 541–551. Retrieved from [https://](https://tc.copernicus.org/articles/11/541/2017/)
647 tc.copernicus.org/articles/11/541/2017/ doi: 10.5194/tc-11-541-2017
- 648 Higashi, A. (1978, jan). Structure and Behaviour of Grain Boundaries in Polycrys-
649 talline Ice. *Journal of Glaciology*, 21(85), 589–605. Retrieved from [https://](https://www.cambridge.org/core/product/identifier/S0022143000033712/type/journal-article)
650 [www.cambridge.org/core/product/identifier/S0022143000033712/type/](https://www.cambridge.org/core/product/identifier/S0022143000033712/type/journal-article)
651 [journal-article](https://www.cambridge.org/core/product/identifier/S0022143000033712/type/journal-article) doi: 10.3189/S0022143000033712
- 652 Howat, I. M., Porter, C., Smith, B. E., Noh, M.-J., & Morin, P. (2019, feb). The

- 653 Reference Elevation Model of Antarctica. *The Cryosphere*, 13(2), 665–674. Re-
 654 trieved from <https://tc.copernicus.org/articles/13/665/2019/> doi: 10
 655 .5194/tc-13-665-2019
- 656 Hruby, K., Gerbi, C., Koons, P., Campbell, S., Martín, C., & Hawley, R. (2020, oct).
 657 The impact of temperature and crystal orientation fabric on the dynamics of
 658 mountain glaciers and ice streams. *Journal of Glaciology*, 66(259), 755–765.
 659 Retrieved from [https://www.cambridge.org/core/product/identifier/
 660 S0022143020000441/type/journal-article](https://www.cambridge.org/core/product/identifier/S0022143020000441/type/journal-article) doi: 10.1017/jog.2020.44
- 661 Hunter, P., Meyer, C., Minchew, B., Haseloff, M., & Rempel, A. (2021). Thermal
 662 controls on ice stream shear margins. *Journal of Glaciology*, 1–15. doi: 10
 663 .1017/jog.2020.118
- 664 Jacka, T. (1984, nov). Laboratory studies on relationships between ice crystal size
 665 and flow rate. *Cold Regions Science and Technology*, 10(1), 31–42. Retrieved
 666 from <https://linkinghub.elsevier.com/retrieve/pii/0165232X84900314>
 667 doi: 10.1016/0165-232X(84)90031-4
- 668 Jacka, T., & Maccagnan, M. (1984, mar). Ice crystallographic and strain rate
 669 changes with strain in compression and extension. *Cold Regions Science and
 670 Technology*, 8(3), 269–286. Retrieved from [https://linkinghub.elsevier
 671 .com/retrieve/pii/0165232X84900582](https://linkinghub.elsevier.com/retrieve/pii/0165232X84900582) doi: 10.1016/0165-232X(84)90058-2
- 672 Jacka, T. H., & Li Jun. (1994). The steady-state crystal size of deforming ice. *An-
 673 nals of Glaciology*, 20(1958), 13–18.
- 674 Jackson, M., & Kamb, B. (1997). The marginal shear stress of Ice Stream B , West
 675 Antarctica. *Journal of Glaciology*, 43(145), 415–426.
- 676 Jacobson, H. P., & Raymond, C. F. (1998, jun). Thermal effects on the location of
 677 ice stream margins. *Journal of Geophysical Research: Solid Earth*, 103(B6),
 678 12111–12122. Retrieved from <http://doi.wiley.com/10.1029/98JB00574>
 679 doi: 10.1029/98JB00574
- 680 Jellinek, H. H. G., & Gouda, V. K. (1969). Grain Growth in Polycrystalline Ice.
 681 *physica status solidi (b)*, 31(1), 413–423. Retrieved from [http://doi.wiley
 682 .com/10.1002/pssb.19690310149](http://doi.wiley.com/10.1002/pssb.19690310149) doi: 10.1002/pssb.19690310149
- 683 Jezek, K., Alley, R., & Thomas. (1985, mar). Rheology of Glacier Ice. *Science*,
 684 227(4692), 1335–1337. Retrieved from [https://www.sciencemag.org/
 685 lookup/doi/10.1126/science.227.4692.1335](https://www.sciencemag.org/lookup/doi/10.1126/science.227.4692.1335) doi: 10.1126/science.227
 686 .4692.1335
- 687 Johnsen, S., Clausen, H. B., Dansgaard, W., Gundestrup, N. S., Hammer, C. U.,
 688 Andersen, U., ... Fisher, D. (1997). The Delta 18O along the Greenland
 689 Ice Core Project deep ice core and the problem of possible Eemian climatic
 690 instability. *Journal of Geophysical Research*, 102(97), 26,397 – 26,410.
- 691 Joughin, I., Rignot, E., Rosanova, C. E., Lucchitta, B. K., & Bohlander, J. (2003,
 692 jul). Timing of Recent Accelerations of Pine Island Glacier, Antarctica. *Geo-
 693 physical Research Letters*, 30(13), 28–31. Retrieved from [http://doi.wiley
 694 .com/10.1029/2003GL017609](http://doi.wiley.com/10.1029/2003GL017609) doi: 10.1029/2003GL017609
- 695 Joughin, I., Smith, B. E., & Medley, B. (2014, may). Marine Ice Sheet Collapse Po-
 696 tentially Under Way for the Thwaites Glacier Basin, West Antarctica. *Science*,
 697 344(6185), 735–738. Retrieved from [https://www.sciencemag.org/lookup/
 698 doi/10.1126/science.1249055](https://www.sciencemag.org/lookup/doi/10.1126/science.1249055) doi: 10.1126/science.1249055
- 699 Karato, S., M., T., & Fujii, T. (1980). Dynamic Recrystallization of Olivine Single
 700 Crystals During High-Temperature Creep. *Geophysical Research Letters*, 7(9),
 701 649–652.
- 702 Ketcham, W. M., & Hobbs, P. V. (1969). An experimental determination of the sur-
 703 face energies of ice. *Philosophical Magazine*, 19(162), 1161–1173. doi: 10.1080/
 704 14786436908228641
- 705 Kuiper, E. J. N., De Bresser, J. H., Drury, M. R., Eichler, J., Pennock, G. M., &
 706 Weikusat, I. (2020). Using a composite flow law to model deformation in the
 707 NEEM deep ice core, Greenland-Part 2: The role of grain size and premelt-

- ing on ice deformation at high homologous temperature. *Cryosphere*, 14(7), 2449–2467. doi: 10.5194/tc-14-2449-2020
- 708 Lee, R. W., & Schulson, E. M. (1988, may). The Strength and Ductility of Ice Under
709 Tension. *Journal of Offshore Mechanics and Arctic Engineering*, 110(2),
710 187–191. Retrieved from [https://asmedigitalcollection.asme.org/
711 offshoremechanics/article/110/2/187/435450/The-Strength-and
712 -Ductility-of-Ice-Under-Tension](https://asmedigitalcollection.asme.org/offshoremechanics/article/110/2/187/435450/The-Strength-and-Ductility-of-Ice-Under-Tension) doi: 10.1115/1.3257049
- 713 Lhermitte, S., Sun, S., Shuman, C., Wouters, B., Pattyn, F., Wuite, J., ... Nagler,
714 T. (2020, oct). Damage accelerates ice shelf instability and mass loss in
715 Amundsen Sea Embayment. *Proceedings of the National Academy of Sciences*,
716 117(40), 24735–24741. Retrieved from [http://www.pnas.org/lookup/doi/
717 10.1073/pnas.1912890117](http://www.pnas.org/lookup/doi/10.1073/pnas.1912890117) doi: 10.1073/pnas.1912890117
- 718 Li, J. C. M., & Chou, Y. T. (1970, may). The role of dislocations in the flow stress
719 grain size relationships. *Metallurgical and Materials Transactions B*, 1(5),
720 1145. Retrieved from <http://link.springer.com/10.1007/BF02900225> doi:
721 10.1007/BF02900225
- 722 Llorens, M.-G., Grier, A., Steinbach, F., Bons, P. D., Gomez-Rivas, E., Jansen,
723 D., ... Weikusat, I. (2017, feb). Dynamic recrystallization during de-
724 formation of polycrystalline ice: insights from numerical simulations.
725 *Philosophical Transactions of the Royal Society A: Mathematical, Phys-
726 ical and Engineering Sciences*, 375(2086), 20150346. Retrieved from
727 <https://royalsocietypublishing.org/doi/10.1098/rsta.2015.0346>
728 doi: 10.1098/rsta.2015.0346
- 729 MacAyeal, D. R. (1989, apr). Large-scale ice flow over a viscous basal sediment:
730 Theory and application to ice stream B, Antarctica. *Journal of Geophys-
731 ical Research: Solid Earth*, 94(B4), 4071–4087. Retrieved from [http://
732 doi.wiley.com/10.1029/JB094iB04p04071](http://doi.wiley.com/10.1029/JB094iB04p04071) doi: 10.1029/JB094iB04p04071
- 733 Meyer, C. R., & Minchew, B. M. (2018, sep). Temperate ice in the shear margins
734 of the Antarctic Ice Sheet: Controlling processes and preliminary locations.
735 *Earth and Planetary Science Letters*, 498, 17–26. Retrieved from [https://
736 doi.org/10.1016/j.epsl.2018.06.028](https://doi.org/10.1016/j.epsl.2018.06.028)[https://linkinghub.elsevier.com/
737 retrieve/pii/S0012821X18303790](https://linkinghub.elsevier.com/retrieve/pii/S0012821X18303790) doi: 10.1016/j.epsl.2018.06.028
- 738 Millstein, J., & Minchew, B. (2020). Inferring ice rheology in Antarctic ice shelves
739 using remotely-sensed surface velocity and ice thickness observations. *AGU
740 Fall Meeting 2020*.
- 741 Montagnat, M., & Duval, P. (2000, nov). Rate controlling processes in the creep of
742 polar ice, influence of grain boundary migration associated with recrystalliza-
743 tion. *Earth and Planetary Science Letters*, 183(1-2), 179–186. Retrieved from
744 <https://linkinghub.elsevier.com/retrieve/pii/S0012821X00002624>
745 doi: 10.1016/S0012-821X(00)00262-4
- 746 Montési, L. G., & Hirth, G. (2003, jun). Grain size evolution and the rheology
747 of ductile shear zones: from laboratory experiments to postseismic creep.
748 *Earth and Planetary Science Letters*, 211(1-2), 97–110. Retrieved from
749 <https://linkinghub.elsevier.com/retrieve/pii/S0012821X03001961>
750 doi: 10.1016/S0012-821X(03)00196-1
- 751 Morlighem, M., Rignot, E., Binder, T., Blankenship, D., Drews, R., Eagles, G., ...
752 Young, D. A. (2020). Deep glacial troughs and stabilizing ridges unveiled
753 beneath the margins of the Antarctic ice sheet. *Nature Geoscience*, 13(2),
754 132–137. Retrieved from <http://dx.doi.org/10.1038/s41561-019-0510-8>
755 doi: 10.1038/s41561-019-0510-8
- 756 Mouginot, J., Scheuch, B., & Rignot, E. (2012). Mapping of ice motion in antarctica
757 using synthetic-aperture radar data. *Remote Sensing*, 4(9), 2753–2767. doi: 10
758 .3390/rs4092753
- 759 Nixon, W., & Schulson, E. (1987, mar). A Micromechanical view of the fracture
760 toughness of ice. *Le Journal de Physique Colloques*, 48(C1), C1–313–C1–319.

- 763 Retrieved from <http://www.edpsciences.org/10.1051/jphyscol:1987144>
764 doi: 10.1051/jphyscol:1987144
- 765 Nixon, W. A., & Schulson, E. M. (1988, may). The Fracture Toughness of Ice
766 Over a Range of Grain Sizes. *Journal of Offshore Mechanics and Arctic Engi-*
767 *neering*, 110(2), 192–196. Retrieved from <https://asmedigitalcollection>
768 [.asme.org/offshoremechanics/article/110/2/192/435461/The-Fracture](https://asmedigitalcollection.asme.org/offshoremechanics/article/110/2/192/435461/The-Fracture-Toughness-of-Ice-Over-a-Range-of)
769 [-Toughness-of-Ice-Over-a-Range-of](https://asmedigitalcollection.asme.org/offshoremechanics/article/110/2/192/435461/The-Fracture-Toughness-of-Ice-Over-a-Range-of) doi: 10.1115/1.3257050
- 770 Ohtomo, M., & Wakahama, G. (1983, oct). Growth rate of recrystallization in
771 ice. *The Journal of Physical Chemistry*, 87(21), 4139–4142. Retrieved
772 from <https://pubs.acs.org/doi/abs/10.1021/j100244a031> doi:
773 10.1021/j100244a031
- 774 Perol, T., & Rice, J. R. (2015, may). Shear heating and weakening of the marg-
775 ins of West Antarctic ice streams. *Geophysical Research Letters*, 42(9), 3406–
776 3413. Retrieved from <http://doi.wiley.com/10.1002/2015GL063638> doi: 10
777 .1002/2015GL063638
- 778 Pollard, D., DeConto, R. M., & Alley, R. B. (2015, feb). Potential Antarctic Ice
779 Sheet retreat driven by hydrofracturing and ice cliff failure. *Earth and Plan-*
780 *etary Science Letters*, 412, 112–121. Retrieved from [http://dx.doi.org/](http://dx.doi.org/10.1016/j.epsl.2014.12.035)
781 [10.1016/j.epsl.2014.12.035](http://dx.doi.org/10.1016/j.epsl.2014.12.035)[https://linkinghub.elsevier.com/](https://linkinghub.elsevier.com/retrieve/pii/S0012821X14007961)
782 [retrieve/pii/S0012821X14007961](https://linkinghub.elsevier.com/retrieve/pii/S0012821X14007961) doi: 10.1016/j.epsl.2014.12.035
- 783 Ranganathan, M., Minchew, B., Meyer, C. R., & Gudmundsson, G. H. (2020, nov).
784 A new approach to inferring basal drag and ice rheology in ice streams, with
785 applications to West Antarctic Ice Streams. *Journal of Glaciology*, 1–14.
786 Retrieved from [https://www.cambridge.org/core/product/identifier/](https://www.cambridge.org/core/product/identifier/S0022143020000957/type/journal%5C%2Farticle)
787 [S0022143020000957/type/journal%5C%2Farticle](https://www.cambridge.org/core/product/identifier/S0022143020000957/type/journal%5C%2Farticle) doi: 10.1017/jog.2020.95
- 788 Rempel, A., & Meyer, C. (2019, jun). Premelting increases the rate of regela-
789 tion by an order of magnitude. *Journal of Glaciology*, 65(251), 518–521.
790 Retrieved from [https://www.cambridge.org/core/product/identifier/](https://www.cambridge.org/core/product/identifier/S0022143019000339/type/journal%5C%2Farticle)
791 [S0022143019000339/type/journal%5C%2Farticle](https://www.cambridge.org/core/product/identifier/S0022143019000339/type/journal%5C%2Farticle) doi: 10.1017/jog.2019.33
- 792 Rignot, E. (2004). Accelerated ice discharge from the Antarctic Peninsula follow-
793 ing the collapse of Larsen B ice shelf. *Geophysical Research Letters*, 31(18),
794 L18401. Retrieved from <http://doi.wiley.com/10.1029/2004GL020697> doi:
795 10.1029/2004GL020697
- 796 Rignot, E., Mouginot, J., & Scheuchl, B. (2011). Ice Flow of the Antarctic Ice Sheet.
797 *Science*, 333(September), 1427–1431.
- 798 Rignot, E., Mouginot, J., & Scheuchl, B. (2017). *MEaSURES InSAR-Based*
799 *Antarctica Ice Velocity Map, Version 2*. Boulder, Colorado USA. NASA
800 National Snow and Ice Data Center Distributed Active Archive Center. doi:
801 <https://doi.org/10.5067/D7GK8F5J8M8R>
- 802 Rignot, E., Vaughan, D. G., Schmelztz, M., Dupont, T., & Macayeal, D. (2002, sep).
803 Acceleration of Pine Island and Thwaites Glaciers, West Antarctica. *Annals of*
804 *Glaciology*, 34, 189–194. Retrieved from [https://www.cambridge.org/core/](https://www.cambridge.org/core/product/identifier/S0260305500256784/type/journal%5C%2Farticle)
805 [product/identifier/S0260305500256784/type/journal%5C%2Farticle](https://www.cambridge.org/core/product/identifier/S0260305500256784/type/journal%5C%2Farticle) doi:
806 10.3189/172756402781817950
- 807 Scambos, T. A. (2004). Glacier acceleration and thinning after ice shelf collapse
808 in the Larsen B embayment, Antarctica. *Geophysical Research Letters*, 31(18),
809 L18402. Retrieved from <http://doi.wiley.com/10.1029/2004GL020670> doi:
810 10.1029/2004GL020670
- 811 Schoof, C. (2007, jul). Ice sheet grounding line dynamics: Steady states, stabil-
812 ity, and hysteresis. *Journal of Geophysical Research*, 112(F3), F03S28. Re-
813 trieved from <http://doi.wiley.com/10.1029/2006JF000664> doi: 10.1029/
814 2006JF000664
- 815 Schulson, E. M., & Hibler, W. D. (1991, jan). The fracture of ice on scales
816 large and small: Arctic leads and wing cracks. *Journal of Glaciology*,
817 37(127), 319–322. Retrieved from <https://www.cambridge.org/core/>

- 818 product/identifier/S0022143000005748/type/journal{_}article doi:
819 10.1017/S0022143000005748
- 820 Schulson, E. M., Lim, P. N., & Lee, R. W. (1984). A brittle to ductile transition
821 in ice under tension. *Philosophical Magazine A: Physics of Condensed Matter,*
822 *Structure, Defects and Mechanical Properties*, 49(3), 353–363. doi: 10.1080/
823 01418618408233279
- 824 Skemer, P., Warren, J. M., Hansen, L. N., Hirth, G., & Kelemen, P. B. (2013).
825 The influence of water and LPO on the initiation and evolution of man-
826 tle shear zones. *Earth and Planetary Science Letters*, 375, 222–233. Re-
827 trieved from <http://dx.doi.org/10.1016/j.epsl.2013.05.034> doi:
828 10.1016/j.epsl.2013.05.034
- 829 Suckale, J., Platt, J. D., Perol, T., & Rice, J. R. (2014, may). Deformation-induced
830 melting in the margins of the West Antarctic ice streams. *Journal of Geophys-*
831 *ical Research: Earth Surface*, 119(5), 1004–1025. Retrieved from [http://doi](http://doi.wiley.com/10.1002/2013JF003008)
832 [.wiley.com/10.1002/2013JF003008](http://doi.wiley.com/10.1002/2013JF003008) doi: 10.1002/2013JF003008
- 833 Thomas, R. H., & Bentley, C. R. (1978). A model for Holocene retreat of the West
834 Antarctic Ice Sheet. *Quaternary Research*, 10(2), 150–170. doi: 10.1016/0033-
835 -5894(78)90098-4
- 836 Thorsteinsson, T., Kipfstuhl, J., & Miller, H. (1997). Textures and fabrics in the
837 GRIP ice core. *Journal of Geophysical Research: Oceans*, 102(C12), 26583–
838 26599. doi: 10.1029/97JC00161
- 839 Tison, J. L., & Hubbard, B. (2000). Ice crystallographic evolution at a temperate
840 glacier: Glacier de Tsanfleuron, Switzerland. *Geological Society Special Publi-*
841 *cation*, 176, 23–38. doi: 10.1144/GSL.SP.2000.176.01.03
- 842 Ultee, L., Meyer, C., & Minchew, B. (2020, dec). Tensile strength of glacial ice
843 deduced from observations of the 2015 eastern Skaftá cauldron collapse, Vat-
844 najökull ice cap, Iceland. *Journal of Glaciology*, 66(260), 1024–1033. Re-
845 trieved from [https://www.cambridge.org/core/product/identifier/](https://www.cambridge.org/core/product/identifier/S0022143020000659/type/journal{_}article)
846 [S0022143020000659/type/journal{_}article](https://www.cambridge.org/core/product/identifier/S0022143020000659/type/journal{_}article) doi: 10.1017/jog.2020.65
- 847 Urai, J., Means, W., & Lister, G. (1995). Dynamic Recrystallization of Minerals.
848 *Geophysical Monograph Series*, 36, 332–347.
- 849 Van der Wal, D., Chopra, P., Drury, M., & Gerald, J. F. (1993). Relationships
850 between dynamically recrystallized grain size and deformation conditions in
851 experimentally deformed olivine rocks. *Geophysical Research Letters*, 20(14),
852 1479–1482. doi: 10.1029/93GL01382
- 853 Van Wessem, J. M., Reijmer, C. H., Morlighem, M., Mouginit, J., Rignot, E., Med-
854 ley, B., . . . Van Meijgaard, E. (2014). Improved representation of East Antarc-
855 tic surface mass balance in a regional atmospheric climate model. *Journal of*
856 *Glaciology*, 60(222), 761–770. doi: 10.3189/2014JoG14J051
- 857 Vaughan, D. G. (1993, jan). Relating the occurrence of crevasses to surface strain
858 rates. *Journal of Glaciology*, 39(132), 255–266. Retrieved from [https://](https://www.cambridge.org/core/product/identifier/S0022143000015926/type/journal{_}article)
859 [www.cambridge.org/core/product/identifier/S0022143000015926/type/](https://www.cambridge.org/core/product/identifier/S0022143000015926/type/journal{_}article)
860 [journal{_}article](https://www.cambridge.org/core/product/identifier/S0022143000015926/type/journal{_}article) doi: 10.1017/S0022143000015926
- 861 Warren, J. M., Hirth, G., & Kelemen, P. B. (2008). Evolution of olivine lattice
862 preferred orientation during simple shear in the mantle. *Earth and Planetary*
863 *Science Letters*, 272(3-4), 501–512. Retrieved from [http://dx.doi.org/](http://dx.doi.org/10.1016/j.epsl.2008.03.063)
864 [10.1016/j.epsl.2008.03.063](http://dx.doi.org/10.1016/j.epsl.2008.03.063) doi: 10.1016/j.epsl.2008.03.063
- 865 Weertman, J. (1974). Stability of the Junction of an Ice Sheet and an Ice Shelf.
866 *Journal of Glaciology*, 13(67), 3–11. doi: 10.3189/s0022143000023327
- 867 Wingham, D. J., Wallis, D. W., & Shepherd, A. (2009). Spatial and temporal evolu-
868 tion of Pine Island Glacier thinning, 1995-2006. *Geophysical Research Letters*,
869 36(17), 5–9. doi: 10.1029/2009GL039126
- 870 Wu, M. S., & Niu, J. (1995). A theoretical analysis of crack nucleation due to grain
871 boundary dislocation pile-ups in a random ice microstructure. *Philosophical*
872 *Magazine A: Physics of Condensed Matter, Structure, Defects and Mechanical*

873 *Properties*, 71(4), 831–854. doi: 10.1080/01418619508236223
874 Zeitz, M., Levermann, A., & Winkelmann, R. (2020). Sensitivity of ice loss to un-
875 certainty in flow law parameters in an idealized one-dimensional geometry.
876 *Cryosphere*, 14(10), 3537–3550. doi: 10.5194/tc-14-3537-2020